



Design and Simulation of a Customized Three-axis Gimbal Structure using Finite Element Analysis Method

Muhammad Amien Kamaruzzaman^{1,*}, Hassrizal Hassan Basri¹, Mohd Nasir Ayob¹

¹ Faculty of Electrical Engineering & Technology, UniMAP, 02600, Perlis, Malaysia

ARTICLE INFO

Article history:

Received 4 January 2023
Received in revised form 26 January 2023
Accepted 17 February 2023
Available online 13 March 2023

Keywords:

Gimbal; Finite Element Analysis;
Computer-Aided Engineering;
SolidWorks

ABSTRACT

This paper presents a Finite Element Analysis (FEA) on a customized three-axis gimbal design application. Examples of applications of the gimbals such as drones, camera stabilizers, and spacecraft. The SolidWorks software checked the gimbal's FEA characteristics with no existing load or normal conditions. Using the FEA method, a static simulation analysis where the material of this assembly design uses Polylactic Acid (PLA), used mainly by 3D printer machines. The force is given to the gimbal structure and obtains the results of the maximum value of stress in MPa, displacement in mm, and strain. Thus, based on the results obtained from SolidWorks, the structure will not fail. The maximum stress value between parts is 2.31 MPa for the support part and 3.09 MPa for the assembly model when the yield stress value of the PLA material properties is at 70 MPa. The new design structure for the gimbal hardware focuses on academic purposes based on PLA material and is easy to build using a 3D printer. In the summary, the customized three-axis gimbal design using SolidWorks will not fracture when the design is in normal condition which has a total force of 6.87 N, which is equal to 0.70 kg at 3.09 MPa where the weight of the base, O-ring, and servo motors at the U-shape part. In addition, the design can hold up to 230.87 N, which is equal to 23.54 kg at 69.90 MPa of the stress value before it will fail at 70 MPa.

1. Introduction

Computer-Aided Engineering (CAE) is widely used by many experts in many sectors, such as agriculture [1] and automotive [2], to improve their product design performance [3] and safety factors [4]. The analysis can be done using the CAE called Finite Element Analysis (FEA). One of the FEA methods is called a Von Mises stress [2, 5, 6]. The Von Mises stress is an analysis that determines the failure criterion on the product design structure and whether it will fracture based on the product material properties. Thus, SolidWorks is one of the CAE software used to design a custom three-axis gimbal as shown in Figure 1 built using PLA material with a yield strength of 70 MPa [7]. The purpose of the gimbal design is for educational design and analysis, which is easy to use and reproduced using the 3D printer by others.

* Corresponding author.

E-mail address: amienkzaman@gmail.com

<https://doi.org/10.37934/araset.30.1.158167>

Gimbal is a device that stabilizes the base part that will always maintain the fixed position without changing the orientation of the base even though the other axis is rotated to another angle. There are three-axis called the roll, pitch, and yaw (x, y, and z) rotation [8]. The common application of gimbals are drones, camera stabilizers, and spacecraft. Nowadays, many people have used these applications in many sectors, such as agriculture, that use drones for their farm and rice fields, the military, and the film industry. The gimbal requires a better structure and controller to have a better performance.

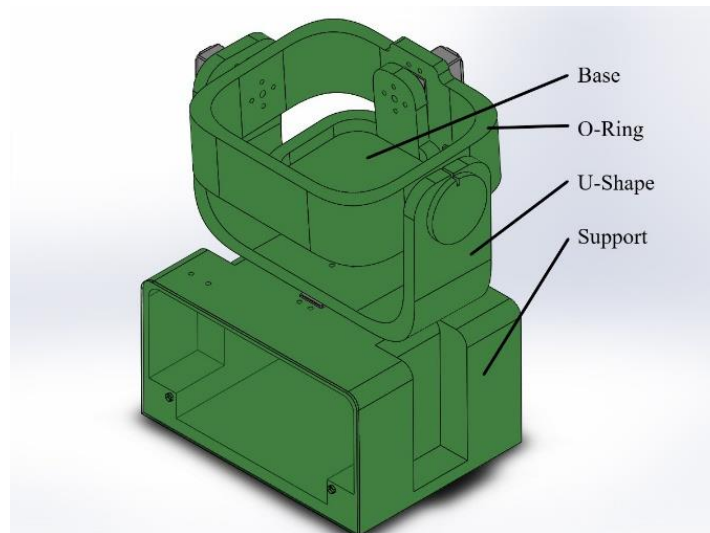


Fig. 1. Assembly model of the gimbal structure

2. Methodology

2.1 Static Simulation Analysis

Static simulation is an FEA analysis applied to the model design in static simulation form where the analysis is not affected over time [9]. It will show the current result based on a given parameter such as force, pressure, and torque [10]. Table 1 shows the PLA material properties that apply to the assembly model. The critical value is at its yield strength, where at maximum value is 70 MPa. This value will be the reference for this analysis on whether it will fracture if the stress result exceeds 70 MPa.

Table 1

PLA material Properties [7]

Properties	Amount
Elastic Modulus (MPa)	3500
Poisson's ratio	0.36
Shear Modulus (MPa)	1287
Mass Density (kg/m^3)	1252
Tensile Strength (MPa)	59
Yield Strength (MPa)	70

Table 2 shows the mechanical design specification of each part's size, thickness, and mass. The value of the mass is obtained from the SolidWorks mass properties feature. The mass properties can generate the current mass of the model design based on the material that applies to the design part. The PLA mass density is the key for this feature, where the value of density of PLA is $1252 kg/m^3$ and the results of the parts are the base is 0.18 kg, O-ring is 0.40 kg, U-shape is 0.36 kg, and support is 1 kg.

Table 2
 Design Parameters for each part

Component Part	Mechanical Specification				
	Length (mm)	Width (mm)	High (mm)	Thickness (mm)	Mass (kg)
(1) Base	100	100	70	10	0.18
(2) O-ring	175	150	70	10	0.40
(3) U-shape	208	70	130	10	0.36
(4) Support	200	150	110	5	1

There are two types of static simulation used for this research static structural analysis. The first study analyzes the assembly model with different values given at two points, as shown in Table 3. The total force of 6.87 N is a condition where there is no external load is given. The second one is an analysis of four different parts with a force of 6.87 N, as shown in Table 4.

Table 3
 Result of stress, displacement, and strain value at different force values at U-shape part

Number	Force Point (N)		Total Force (N)	Mass (kg)	σ , Stress (MPa)	u , Displacement (mm)	ϵ , Strain
	Left	Right			Max Value	Max Value	Max Value
1	3.73	3.14	6.87	0.70	3.09	0.11	0.0014
2	53.73	53.14	106.87	10.89	31.60	0.78	0.0147
3	103.73	103.14	206.87	21.09	62.50	1.54	0.0290
4	115.73	115.14	230.87	23.54	69.90	1.72	0.0325
5	153.73	153.14	306.87	31.28	93.40	2.31	0.0434

Table 4
 Result of stress, displacement, and strain values between four parts

Component Part	Force Point (N)		Total Force (N)	Mass (kg)	σ , Stress (MPa)	u , Displacement (mm)	ϵ , Strain
	Left	Right			Max Value	Max Value	Max Value
(1) Base	-	-	-	0.18	4.51×10^{-5}	0.081	1.21×10^{-8}
(2) O-ring	-	-	-	0.40	0.129	0.103	3.11×10^{-5}
(3) U-shape	3.73	3.14	6.87	0.36	0.488	0.107	1.26×10^{-4}
(4) Support	-	-	-	1	2.310	0.023	9.16×10^{-4}

2.2 Method

Figure 2 shows the flowchart of the method implemented in this research. The first step is to draw each part of the gimbal structure, the base, O-ring, U-shape, and support part, with the accurate measurement for bolt and nut holes and servo slot. The next step is to assemble the parts into one complete model. After that, start the static simulation study with the connection of part is clarify which is bolt and nut. Then, clarify the force as shown in Figure 3, where the two points are given at the U-shape part, 3.73 N at the left point and 3.14 N at the right point.

Lastly, the results will be obtained from the analysis as shown in Table 3 and Table 4. The stress, displacement, and strain will be obtained with two different data results, the first one at assembly with different force values as shown in Table 3. The second one is different parts with the same force as shown in Table 4.

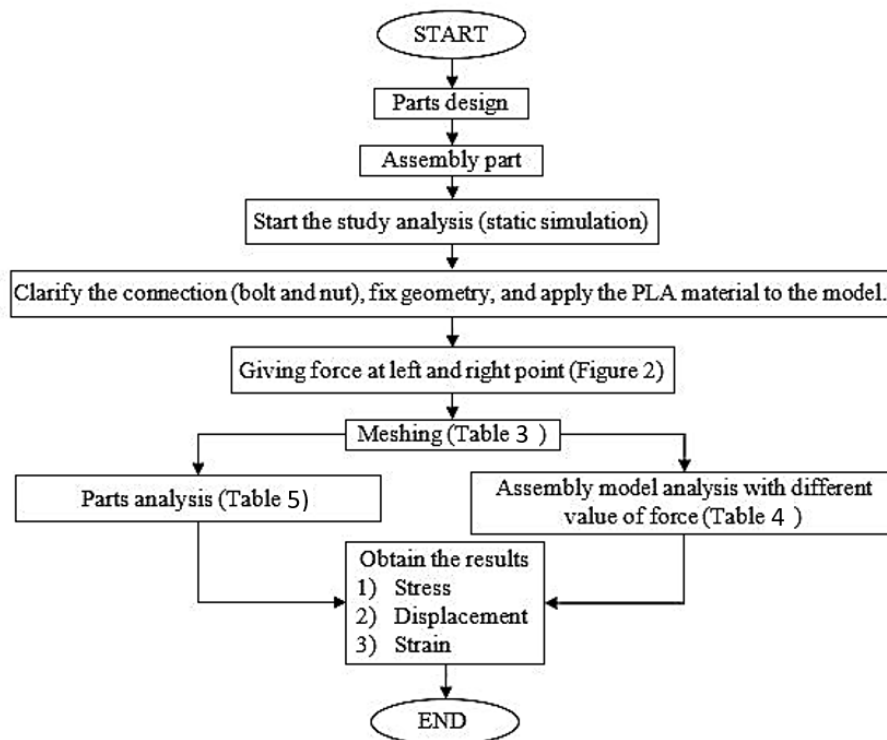


Fig. 2. Step of simulation analysis study flowchart

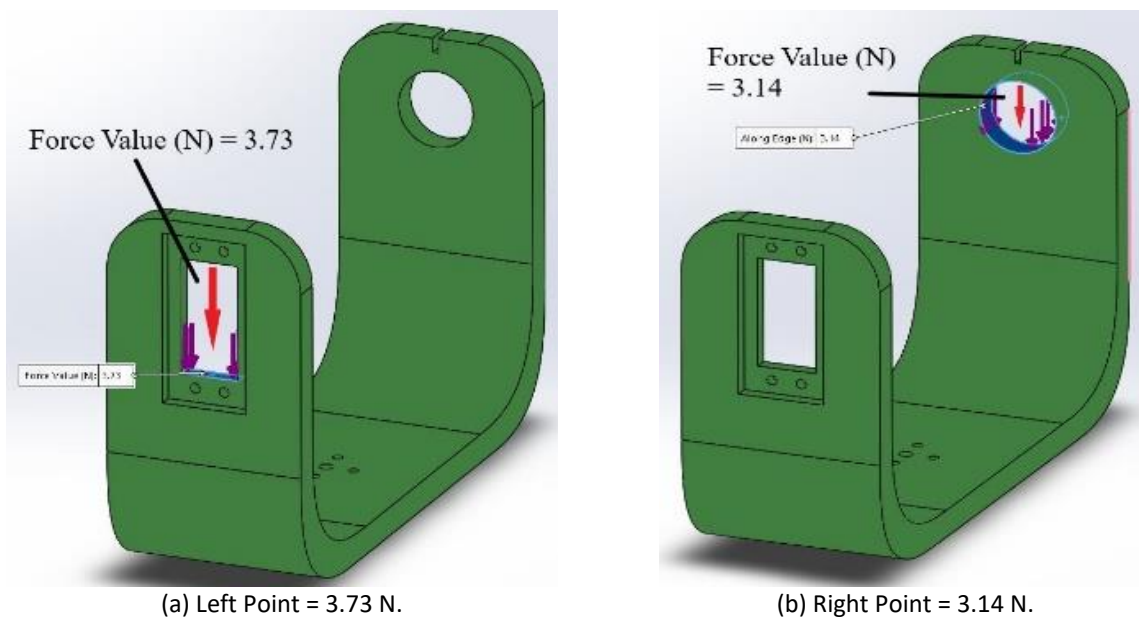


Fig. 3. Location of 2 points given, where total force is equal to 6.87 N (weight of the two servo motors, O-ring, and base parts)

2.3 Force Point on U-Shape Part

Figure 3 shows the exact point at the U-shape model of the gimbal assembly model. This force value is obtained by using Eq. 1. The left point is equal to 3.73 N and the right point is equal to 3.14 N considering the weight of the servo motors (60 g), O-ring, and base parts.

$$F = mg \tag{1}$$

F is a force value in newton, m is a mass in kilogram, and g is gravity equal to 9.81ms^{-2} . The value of force is obtained after the total weight of the base, O-ring, and servo motors are obtained, which is equal to 0.64 kg and divided by two since each point uses the exact weight of the base, O-ring, and servo motor. Figure 3(a) has more force value than the right point because there is another servo motor attached to the U-shape where the mass of the servo motor is 60 g. Thus, the left point is required to add the weight of another servo motor.

3. Results

3.1 Assembly Result

The results of stress, displacement, and strain of the assembly model and parts model are obtained using the SolidWorks simulation study feature [17-20]. Table 3 shows the analysis result for the U-shape part with a different value of forces. Since the PLA yield stress is at 70 MPa, when the force is at 206.87 N, equal to 21.09 kg, the assembly model will not fracture since the maximum stress is 62.50 MPa. The maximum force value that the gimbal can hold is 230.87 N, equal to 23.54 kg. If the force exceeds 230.87 N, the structure will fracture and fail. For example, when the force value is at 306.87 N, equal to 31.28 kg, the gimbal assembly will fracture because the maximum stress value is 93.40 MPa which is above the maximum yield value of the PLA material which is 70 MPa. Figure 4 shows the stress vs total force graph that visualizes the results from Table 3.

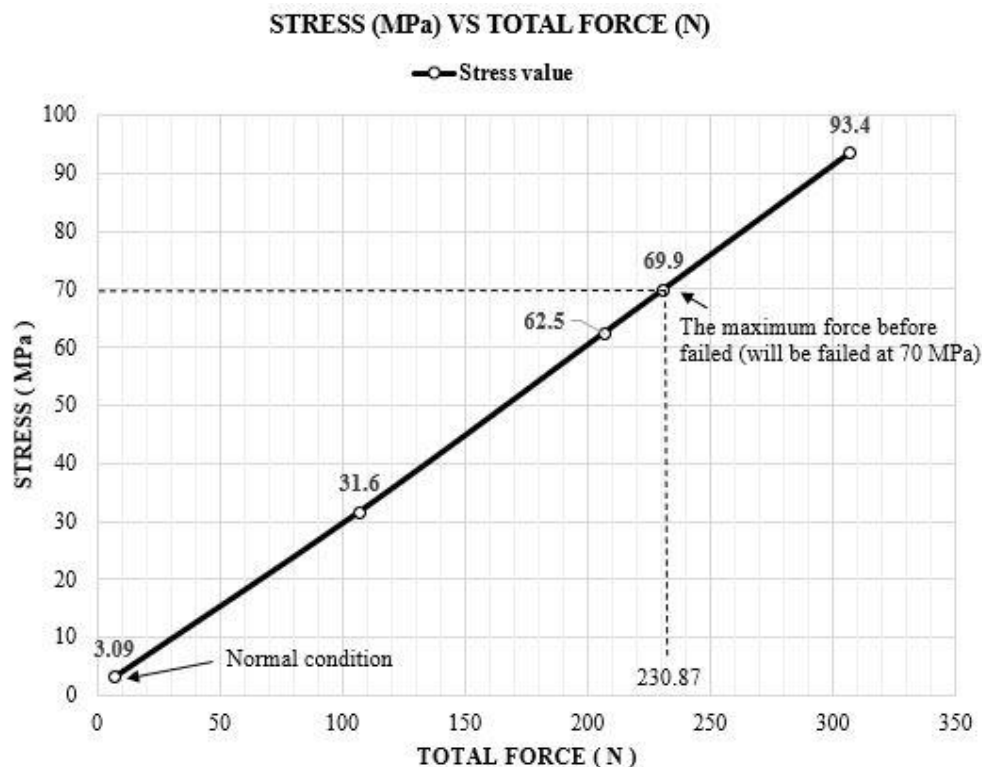


Fig. 4. Stress vs total force graph result

Figure 5 shows the stress, displacement, and strain based on Table 3. At the force value of 6.87 N, the maximum stress is 3.09 MPa. The maximum displacement is 0.11 mm, and the 0.0014 strain value. This shows that when the assembly model is at the force of 6.87 N, the displacement result is at 0.11 mm, less than 1mm. This error is very small compared to other force values. When the value of force is higher, the stress, displacement, and strain will be higher.

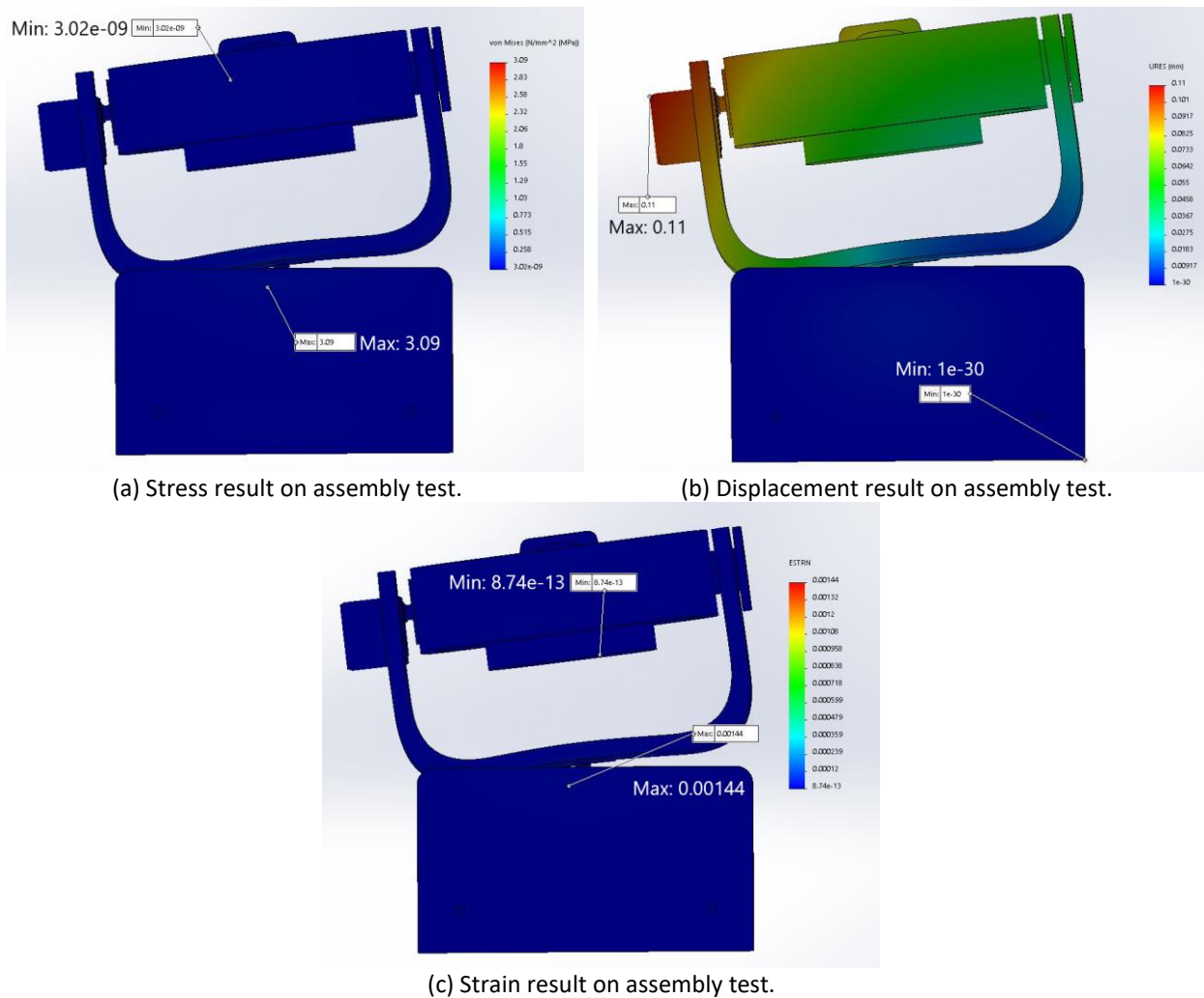


Fig. 5. The stress, displacement, and strain results of the assembly simulation test

3.2 Result Between The Four Parts

The Table 4 shows the results obtained from four different parts of the gimbal assembly model which are the base, O-ring, U-shape, and support.

Figure 6 shows the stress result between the four parts. The maximum stress value is at the support part at 2.31 MPa. There is a huge difference in the stress value from the other parts. Even though the force is at the U-shape, the value of stress at the U-shape is smaller than the support part, which is 0.488 MPa. Thus, for the most part, that effect is the support part and still not fracture.

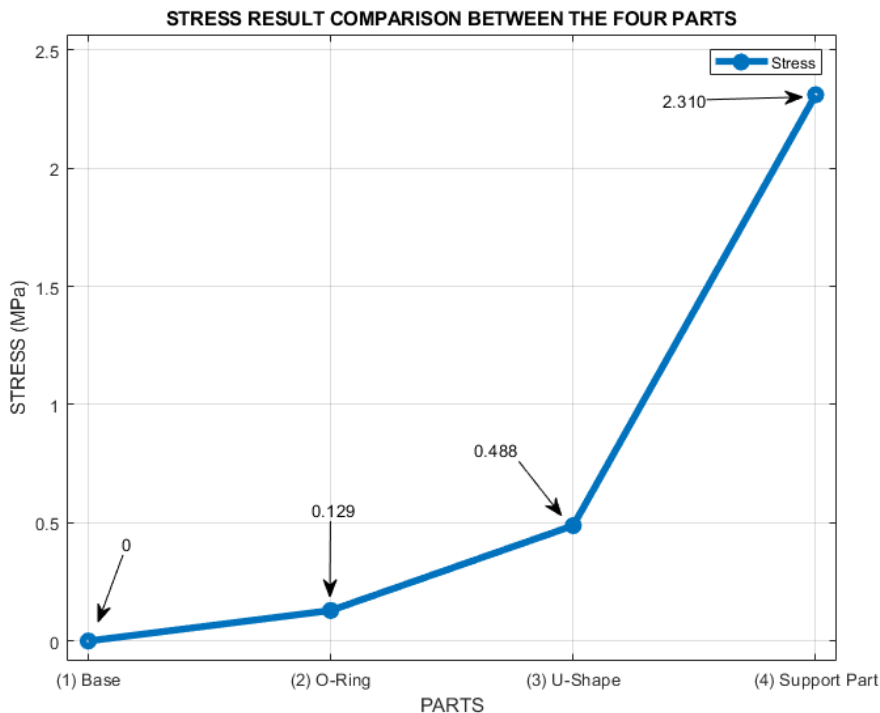


Fig. 6. Stress results in four different parts

Figure 7 shows the displacement of the four parts. The given force point is at the U-shape part, so clearly that the higher displacement value is at the U-shape part at 0.107 mm and 0.103 mm for O-ring since this part is attached to the U-shape part. The most lower of displacement error is the support part at 0.023 mm.

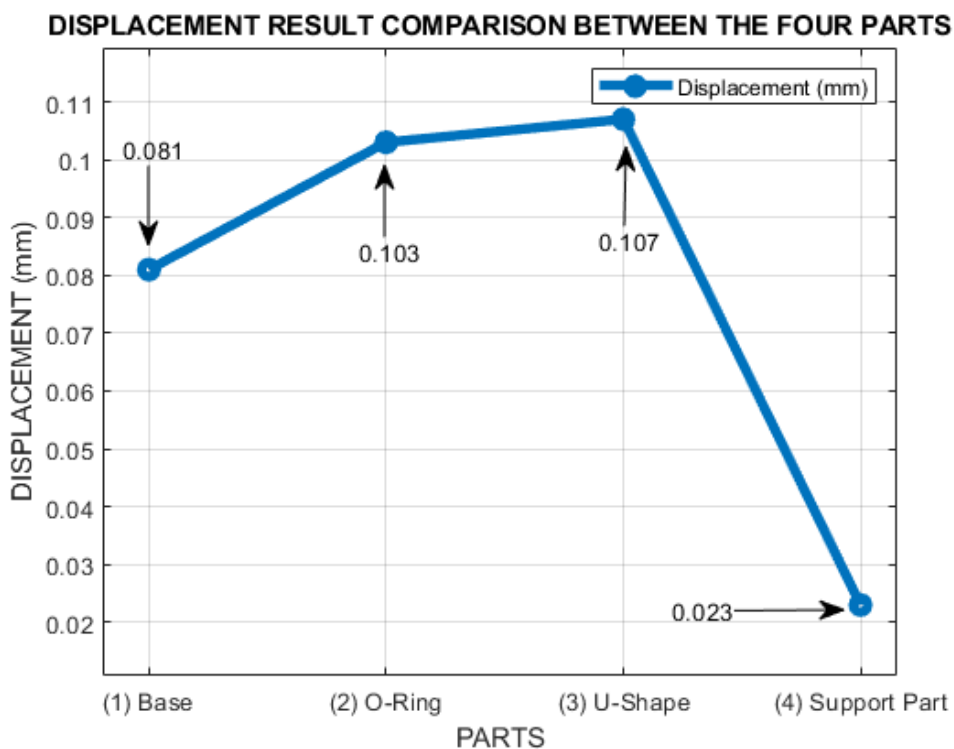


Fig. 7. Displacement results between four different parts

Figure 8 shows the strain result between four different parts. The most higher strain value occurs at the support part at 9.16×10^{-4} . The lowest strain value is the base part at 1.21×10^{-8} .

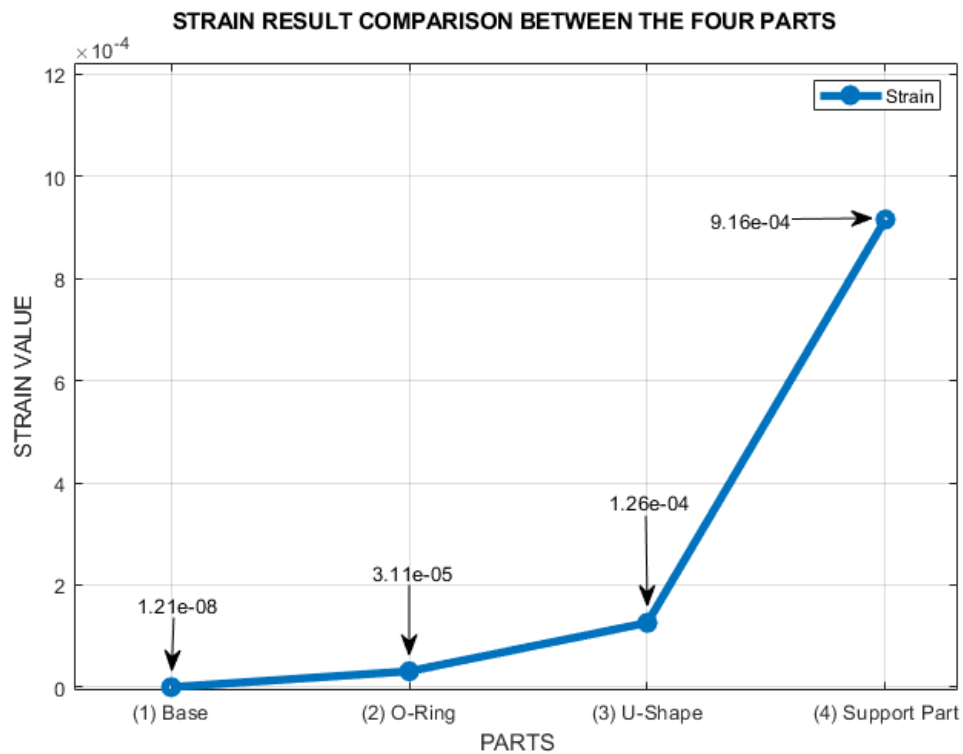


Fig. 8. Strain results between four different parts

3.3 Meshing Process

Meshing is a method that subdivides the assembly model into small pieces [11-16]. In design analysis, meshing is an important step that needs to be considered. When the mesh of the assembly part is more detailed, the more accurate the simulation result will be. Table 5 shows the element size of the meshing process for this gimbal structure, where the maximum value is 6.91 mm, and the minimum is 0.35 mm. The meshing type used is curvature-based mesh.

Table 5

Meshing details of the assembly analysis obtain from SolidWorks

Mesh Details	Data Information
Mesh Type	Solid Mesh
Mesher Used	Curvature-based mesh
Jacobian Points	4 Points
Max Element Size	6.90637 mm
Min Element Size	0.345319 mm
Mesh Quality	High
Total Nodes	931199
Total Elements	602604
Maximum Aspect Ratio	4.12×10^5
Percentage of elements with Aspect Ratio < 3	94
Percentage of elements with Aspect Ratio > 10	0.473

4. Discussion

The most crucial part is that the simulation study needs to clarify the connection between each part. For example, the servo motor is connected to the O-ring part using a bolt and nut with dimension size of 3 mm or M3. The second one is the meshing process. When the geometry of the design is more complex, sometimes it will be hard to mesh simultaneously in the assembly model if the size of meshing is not suitable for certain parts. Next, the material properties are also important to run a static simulation and have an accurate result. If the material properties are wrong, the result might be not valid. Thus, the selection of material properties details is important so that the result of stress, displacement, and strain is accurate.

5. Conclusions

In conclusion, the new structure of the three-axis gimbal can be used for the experimental test since the result shows that the strength of the structure is not failed by using the finite element analysis method on SolidWorks. The results show when a certain force is given to these two points, the maximum force is able up to 230.87 N, which is equal to 23.54 kg at 69.90 MPa of the stress value. The yield value for the PLA material is around 70 MPa. Thus, when this structure is in a normal position which means no load is given, the stress value is 3.09 MPa on assembly model analysis. This shows the current design can prove that this structure will not fracture.

Acknowledgement

This research was supported by the Ministry of Higher Education, Malaysia, through the Fundamental Research Grant Scheme (Ref: FRGS/1/2020/TK0/UNIMAP/03/34). The authors also acknowledge the Faculty of Electrical Engineering, Universiti Malaysia Perlis (UniMAP) for the equipment and technical assistance.

References

- [1] Patuk, Iaroslav, and Piotr F. Borowski. "Computer aided engineering design in the development of agricultural implements: a case study for a DPFA." In *Journal of Physics: Conference Series*, vol. 1679, no. 5, p. 052005. IOP Publishing, 2020. <https://doi.org/10.1088/1742-6596/1679/5/052005>
- [2] Ren, Yuan, Yongchang Yu, Binbin Zhao, Chuanhui Fan, and He Li. "Finite element analysis and optimal design for the frame of SX360 dump trucks." *procedia engineering* 174 (2017): 638-647. <https://doi.org/10.1016/j.proeng.2017.01.201>
- [3] Kwon, Hyuk-Jae, and Hong-Kyu Kwon. "Computer aided engineering (CAE) simulation for the design optimization of gate system on high pressure die casting (HPDC) process." *Robotics and Computer-Integrated Manufacturing* 55 (2019): 147-153. <https://doi.org/10.1016/j.rcim.2018.01.003>
- [4] Cholette, Michael E., Pietro Borghesani, Egidio Di Galleonardo, and Francesco Braghin. "Using support vector machines for the computationally efficient identification of acceptable design parameters in computer-aided engineering applications." *Expert Systems with Applications* 81 (2017): 39-52. <https://doi.org/10.1016/j.eswa.2017.03.050>
- [5] Darmawan, Agung Setyo, Junaidi Syarif, Pramuko Ilmu Purboputro, Agus Yulianto, Abdul Hamid, and Noviyanto Noviyanto. "Single friction plate clutch design for cars with power of 77 kW and speed of 6000 rpm using finite element method." *Applied Research and Smart Technology (ARSTech)* 1, no. 1 (2020): 22-27. <https://doi.org/10.23917/arstech.v1i1.33>
- [6] Nordin, Nurul Hazirah, Nurul Akmal Naamandadin, Wan Azani Mustafa, and Norrazman Zaiha Zainol. "Stress Analysis of Urban Solid Waste Trap by Using Finite Element Analysis (FEA)." *Journal of Advanced Research in Applied Mechanics* 53, no. 1 (2019): 1-7.
- [7] Farah, Shady, Daniel G. Anderson, and Robert Langer. "Physical and mechanical properties of PLA, and their functions in widespread applications—A comprehensive review." *Advanced drug delivery reviews* 107 (2016): 367-392. <https://doi.org/10.1016/j.addr.2016.06.012>

- [8] Altan, Aytaç, and Rifat Hacıoğlu. "Model predictive control of three-axis gimbal system mounted on UAV for real-time target tracking under external disturbances." *Mechanical Systems and Signal Processing* 138 (2020): 106548. <https://doi.org/10.1016/j.ymssp.2019.106548>
- [9] Ren, Jie, Jian Wang, Shirong Guo, Xing Li, Kunpeng Zheng, and Zhe Zhao. "Finite element analysis of the static properties and stability of a large-span plastic greenhouse." *Computers and Electronics in Agriculture* 165 (2019): 104957. <https://doi.org/10.1016/j.compag.2019.104957>
- [10] Venugopal, Arvinthan, Roslina Mohammad, and Md Fuad Shah Koslan. "Fatigue Crack Growth Prediction on Su-30MKM Horizontal Stabilizer Lug Using Static Analysis." *Journal of Advanced Research in Applied Mechanics* 99, no. 1 (2022): 10-23.
- [11] Karakan, İsmet, Ceren Gürkan, and Cem Avci. "Performance analyses of mesh-based local Finite Element Method and meshless global RBF Collocation Method for solving Poisson and Stokes equations." *Mathematics and Computers in Simulation* 197 (2022): 127-150. <https://doi.org/10.1016/j.matcom.2022.02.015>
- [12] Ni, Tao, Qi-zhi Zhu, Lun-Yang Zhao, and Peng-Fei Li. "Peridynamic simulation of fracture in quasi brittle solids using irregular finite element mesh." *Engineering Fracture Mechanics* 188 (2018): 320-343. <https://doi.org/10.1016/j.engfracmech.2017.08.028>
- [13] Zhang, Yancheng, Gildas Guillemot, Marc Bernacki, and Michel Bellet. "Macroscopic thermal finite element modeling of additive metal manufacturing by selective laser melting process." *Computer Methods in Applied Mechanics and Engineering* 331 (2018): 514-535. <https://doi.org/10.1016/j.cma.2017.12.003>
- [14] Chen, Wenjiong, Xiaonan Zheng, and Shutian Liu. "Finite-element-mesh based method for modeling and optimization of lattice structures for additive manufacturing." *Materials* 11, no. 11 (2018): 2073. <https://doi.org/10.3390/ma11112073>
- [15] Yaakob, Yusli, Mahamad Hisyam Mahamad Basri, Muhammad Farhan Bardzan, Noor Iswadi Ismail, Azli Abd Razak, and Muhammad Arif Ab Hamid Pahmi. "The Stability Analysis Of Floating Buoy As A Wave Energy Harvester For Malaysian Coastal Area." *Journal of Advanced Research in Applied Mechanics* 96, no. 1 (2022): 1-6. <https://doi.org/10.37934/aram.96.1.16>
- [16] Jalil, Nawal Aswan Abdul, Hussein Kadhim Sharaf, and Sadeq Salman. "A simulation on the effect of ultrasonic vibration on ultrasonic assisted soldering of Cu/SAC305/Cu joint." *Journal of Advanced Research in Applied Mechanics* 36, no. 1 (2017): 1-9.
- [17] Mulyana, Tatang, Darwin Sebayang, Fildzah Fajrina, and M. Faizal. "Design and analysis of solar smartflower simulation by solidwork program." In *IOP Conference Series: Materials Science and Engineering*, vol. 343, no. 1, p. 012019. IOP Publishing, 2018. <https://doi.org/10.1088/1757-899X/343/1/012019>
- [18] Mulyana, Tatang, Darwin Sebayang, H. D. Jauharah, and M. Yahya Shomit. "Design and Analysis of Windmill Simulation and Pole by Solidwork Program." In *IOP Conference Series: Materials Science and Engineering*, vol. 343, no. 1, p. 012018. IOP Publishing, 2018. <https://doi.org/10.1088/1757-899X/343/1/012018>
- [19] Shen, Cheng, Shixun Fan, Xianliang Jiang, Ruoyu Tan, and Dapeng Fan. "Dynamics Modeling and Theoretical Study of the Two-Axis Four-Gimbal Coarse–Fine Composite UAV Electro-Optical Pod." *Applied Sciences* 10, no. 6 (2020): 1923. <https://doi.org/10.3390/app10061923>
- [20] Kunalan, Kerishmaa Theavy, Cheng Yee Ng, and Nauman Riyaz Maldar. "A performance investigation of a multi-staging hydrokinetic turbine for river flow." *Progress in Energy and Environment* 17 (2021): 17-31. <https://doi.org/10.37934/progee.17.1.1731>